Non-Hermitian Quasiperiodic SSH Ladder

Si-Yu Yuan*
Department of Physics, National University of Singapore, Singapore 117551, Singapore
(Dated: November 16, 2024)

Topological matters in non-Hermitian region have attracted much attention in the recent few years. However, there is a cluster of less-known emergent models called non-Hermitian quasicrystals (nHQCs). And it is a natural extension to introduce conventional topological edge states into nHQCs. The interplay of non-Hermiticity, topology and disorder remains intriguing. Here, we present a detailed study on a non-Hermitian quasiperiodic Su-Schrieffer-Heeger (SSH) ladder model, which incorporates quasiperiodic complex-valued interchain couplings. This model combines non-Hermitian physics, topological edge states, and quasiperiodicity, revealing rich phase transitions characterized by winding numbers and unique symmetry-stabilized zero modes. Aside from mapping out the metal-insulator transitions, we also uncover a non-Hermitian Hofstadter butterfly pattern driven by quasiperiodic modulations. Our results provide insights into non-Hermitian quasicrystal phases, extend the understanding of novel topological states with coexistence of the above fancy ingredients.

INTRODUCTION

Recent developments in non-Hermitian topological systems have unveiled unconventional phenomena such as the non-Hermitian skin effect, complex bulk-boundary correspondence, and unique topological phases [1]. Non-Hermitian models, where Hamiltonians are extended with complex onsite potentials or asymmetric hoppings, exhibit these features as a result of gain and loss in open classic or quantum systems, making them fundamentally different from Hermitian systems. The study of non-Hermitian systems has expanded to quasicrystals, which display long-range order without periodicity, providing a new platform for observing metal-insulator transitions and localized states in a topologically rich setting.

As one of the basic models with non-trivial topological properties, the celebrated Su-Schrieffer-Heeger (SSH) model serves as a critical building block in condensed matter physics [2]. A cluster of higher-order topological states can be observed by simply stacking SSH model in higher dimensions [3, 4]. While a paradigmatic model predicting the existence of localization transition in quasiperiodic one-dimensional (1D) chain is the Aubry-André-Harper (AAH) model [5]. It is obtained by dimension reduction of a effective two-dimensional (2D) model with magnetic flux, thus can be characterized by Chern number, which makes it exceptional in 1D models. Hereby we propose a intriguing model that combines topological zero modes with the localization-delocalization transition originated from both non-Hermiticity and quasiperiodicity, namely the non-Hermitian quasiperiodic SSH ladder.

The aim of our research is to investigate a SSH ladder with complex quasiperiodic interchain couplings, which introduces a hybridization of multiple desired properties. This setup bridges topological non-Hermitian physics and quasicrystals, revealing a rich phase structure, including metal-insulator transitions which can be predicted by winding numbers, topological zero modes stabilized by non-Hermitian chiral symmetry (nHCS), and a non-Hermitian version of the Hofstadter butterflies, one of the most renowned examples of fractals in condensed matter physics. The robustness of pinned zero modes is verified by the Hofstadter butterflies under various kind of symmetry-preserving modulations.

MODEL AND GENERAL THEORY

There are many ways to introduce non-Hermiticity and quasiperiodicity to the SSH ladder. Here the system of interest is two relatively shifted SSH chains with complex AAH-like interchain coupling. This sort of configuration respects particle-hole ($\mathcal{CP}$) symmetry in the Hermitian limit, while non-Hermitian chiral symmetry enforcing center-symmetric eigenvalue pairs (eigenvalues) is preserved when we turn on the imaginary coupling [6–8], thus presents symmetry-stabilized topological zero modes, while the non-Hermitian quasiperiodic coupling provides us a transition from delocalized states to localized states.

Despite the quasiperiodicity, a unit cell for SSH ladder is composed of four fermions, as shown in Fig. 1. In the ith unit cell, a_i and b_i are the fermion annihilation operators in the upper leg, while A_i, B_i are those of the opposite leg. When we turn on the non-Hermitian quasiperiodic interchain coupling, the real space Hamiltonian is given by

$$\begin{aligned} H = &\sum_i [t_1(b_i^\dagger a_i + A_{i+1}^\dagger B_i) + t_2(a_{i+1}^\dagger b_i + B_i^\dagger A_i) + H.c.] \\ &+ \sum_i (\mu_{2i-1} a_i^\dagger A_i + \mu_{2i} b_i^\dagger B_i + H.c.), \end{aligned} \tag{1}$$

where $\mu_n = \mu_0 \cos(2\pi\tau n + \phi)$ is the quasiperiodic interchain coupling strength that breaks translational in-

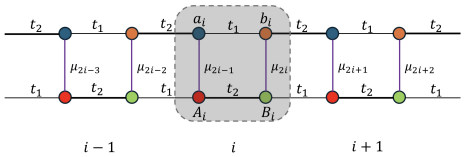

FIG. 1. Schematic diagram for the non-Hermitian quasiperiodic SSH ladder lattice

variance and introduces a landscape in coupling strength that mirrors non-Hermitian analogs of the AAH model. The non-Hermiticity is introduced by the complex phase $\phi = \theta + \mathrm{i}h$ following Ref. [9–11], and θ is fixed at zero for the sake of nHCS, which also contributes to the reason we get rid of quasiperiodic onsite potential. Since the topological phases in conventional coupled SSH systems are well settled [12], we are not attempting to figure out the topological phase transition brought about by t_1/t_2. The values, $t_1 = \frac{1}{2}$, $t_2 = 2$, and $\mu_0 = 2$, are cautiously chosen, which lies in the topological non-trivial region in the Hermitian limit.

Here we are interested in the bulk properties and aimed at capturing localization transition in the thermal dynamic limit, that is, the characteristic system size $L \to \infty$. Notice that any irrational value τ can be approximately expressed by a sequence of rational numbers p_n/q_n, where p_n, q_n are prime integers that go to infinity as $n \to \infty$ [13]. To mimic a truly infinitely large system in numeric simulations, we can chose a finite number of sites $L = q_n/2$ and apply periodic boundary condition (PBC), $\psi_{n+L,c} = \psi_{n,c}$ (c represents the fermions in one unit cell in the periodic limit). In the following calculations, $\tau = \frac{\sqrt{5}-1}{2}$ is the inverse of the golden mean, L is set to be 305 because $\tau \approx 377/610$ and each cell contains two non-identical interchain couplings.

METAL-INSULATOR TRANSITION

The localization transition is also called metal-insulator transition (MIT), in the sense that the 'metal' phases refer to the ones whose eigenstates are extended while the eigenstates of 'insulator' phases are localized. In non-Hermitian quasicrystals, MITs are driven by adiabatically varying both imaginary phase h and the quasiperiodic coupling strength μ_0. In our model, we analyze the transition by fixing the coupling strength while observing the localization of eigenstates under different non-Hermitian phases. To characterize the transition, we apply the inverse participation ratio (IPR), calculated as

$$IPR = \sum_n \frac{|\psi_n|^4}{(\sum_n |\psi_n|^2)^2}, \tag{2}$$

with $IPR \simeq 1/L \simeq 0$ yielding a extended state and $IPR \simeq 1$ for fully-localized state. As the value of the non-Hermitian phase increases, the system transitions from a metallic phase to an insulating phase, indicating localization. By numerically evaluate the IPRs, like Fig. 2(c), it is obvious to observe the MIT. When we fine tune the complex phase h, the imaginary part of the spectrum are growing gradually, as indicated in Fig. 2(a). The phase transition is also marked by the two segments of maximum absolute values of imaginary eigenenergy ($\max\{|\mathrm{Im}[E]|\}$) with totally different slopes, distinguishing the metallic and insulating phases (see Fig. 2(b)).

To predict the critical point in the transition, the winding number is defined as [11]

$$\nu = \lim_{L\to\infty} \frac{1}{2\pi\mathrm{i}} \int_0^{2\pi} \mathrm{d}\theta \frac{\partial}{\partial\theta} \log\det\left\{H(\frac{\theta}{L}, h) - E_{ref}\right\}. \tag{3}$$

While zero windings indicate metallic phases, ν acquires non-trivial value (-1) when the system enters insulating phase. The numerically computed winding numbers are shown as Fig. 2(f), the critical point $h_c \approx 0.69$ matches well with the abrupt changes in IPRs and the non-Hermitian energy spectrum. Also, the IPRs and maximum $|\mathrm{Im}[E]|$ under open boundary condition (OBC) are worthy of notice. Due to the well-known breakdown of PBC-OBC spectrum correspondence in non-Hermitian physics, the transition in OBC spectra fails to fall in line with the PBC ones as predicted by the windings, showcased as Fig. 2(d). However, most OBC eigenstates preserves the same critical behaviors in IPR, except the robust topological zero modes, which give us relatively high IPRs across the whole range of h (Fig. 2(e)). Although the winding number ν is not capable of capture the topological zero modes as its conventional Hermitian counterparts do, it describes the bulk properties and provides a faithful prediction on MIT. There is also a probability that we can obtain the critical point h_c analytically through a similarity transformation, like indicated in Ref. [11].

NON-HERMITIAN HOFSTADTER BUTTERFLY AND SYMMETRY-STABILIZED ZERO MODES

The quasiperiodic coupling μ_n introduces fractal energy band structures, manifesting as a non-Hermitian analog of the Hofstadter butterfly. The structure arises by plotting the eigenvalues as a function of the modulated flux ratio τ, capturing the fractal nature of the energy spectrum due to continuously tuning τ through

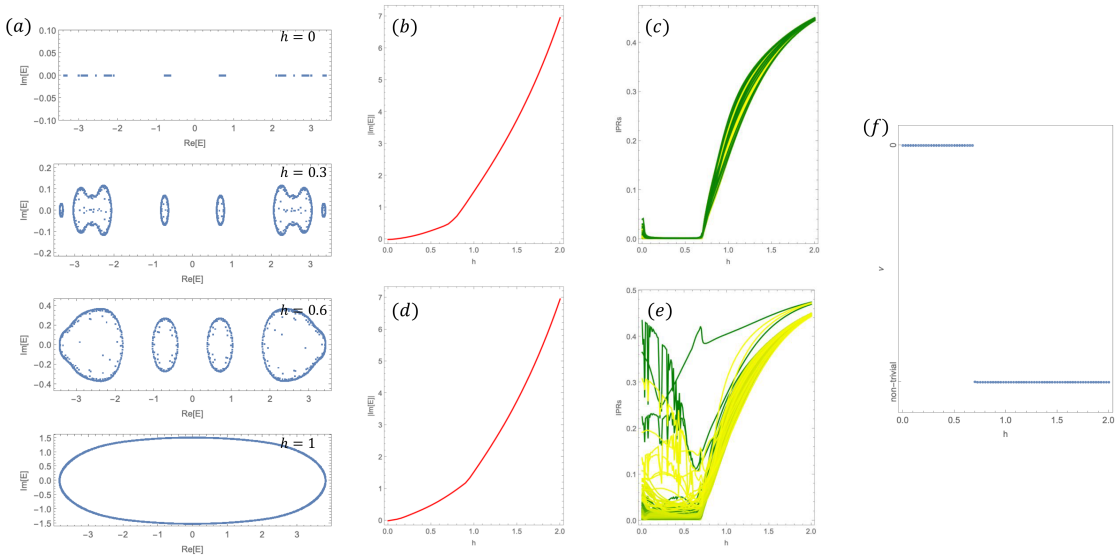

FIG. 2. Metal-insulator transition in the non-Hermitian quasiperiodic SSH ladder Hamiltonian $H(\theta, h)$ for $t_1 = \frac{1}{2}$, $t_2 = 2$, $\mu_0 = 2$, and $\tau = (\sqrt{5}-1)/2$. PBC is assumed on a lattice with $L = 305$ for (a)-(c) and (f). (d) and (e) are plotted under OBC at $L = 250$. (a) Complex eigenenergy spectrum for a few increasing values of the complex phase h. (b) Scaling of $\max\{|\mathrm{Im}[E]|\}$ versus non-Hermitian phase h. Different tendencies can be observed on both sides of the critical value $h_c \approx 0.69$. (c) Numerically-computed inverse participation ratios of eigenstates. (d) Behavior of $\max\{|\mathrm{Im}[E]|\}$ versus h. No correspondence with the transition point. (e) Numerically-computed IPRs of eigenstates under OBC. Localization anomaly emerges for topological edge states. (f) Numerically-computed winding numbers. E_{ref} is set to be zero. While the non-trivial values are not convergent to -1 due to the small system dimension used, they give relatively good prediction on h_c.

quasiperiodic and periodic modulations with respect to the underlying lattice.

In general, the eigenenergies become complex in the non-hermitian cases, leading to a three-dimensional non-Hermitian version of Hofstadter butterfly, as plotted in Fig. 3. We identify different spectral patterns, in weak non-Hermiticity limit, the real part of the spectrum resembles a butterfly pattern, representing complex fractal structures akin to the Hofstadter butterfly found in Hermitian quasiperiodic models. Specially, when $h = 0$, the spectra is confined in the real plane (see Fig. 3(d)). While in insulating phase, the butterfly pattern no longer exists, and the zero modes are eliminated by large h (Fig. 3(e)). Here, non-Hermiticity introduces a new dimension where the imaginary components of the spectrum encode the degree of localization in different phases. Complex spectral flow emerges in both phases, which remains inviting to be explored.

Zero-energy modes are of particular interest in topological insulators, as they are always associated with boundary states protected by symmetries. In the non-Hermitian SSH ladder model, though $\mathcal{CP}$ symmetry is lifted boiled down to the non-Hermitian phase, we find that certain parameter regimes yield topological edge modes pinned at zero energy by a non-Hermitian chiral symmetry constructed by using the product of parity-time symmetry and non-Hermitian particle-hole symmetry [6–8]. Unlike the commonly-seen six basic symmetries in non-Hermitian physics, nHCS, one of the non-Hermitian gauged symmetries, guarantees the spectrum symmetric about the origin of the complex energy plane. It can be easily verified by applying symmetry-breaking perturbations, for example, a non-vanishing onsite potential $\delta a_i^\dagger a_i$ can annihilate the coalesce of topological modes.

Also, there is an interesting phenomenon that the zero modes can survive and even be recovered by floquet modulation. In this circumstance, the symmetry-preserving interchain coupling is rewritten as

$$\mu_n = \mu_0 \cos(2\pi\tau n + \phi)\cos(\omega t). \tag{4}$$

Now the interchain coupling is under periodic driving, with period $T = 2\pi/\omega$, where ω is the driving frequency. We can compute the qusaienergy and show that their is another kind of analog to Hofstadter butterfly, namely the floquet non-Hermitian Hofstadter butterfly. The calculation is performed numerically adopting the split-operator method. The evolution can be divided in N steps, with N being a sufficiently large number. The

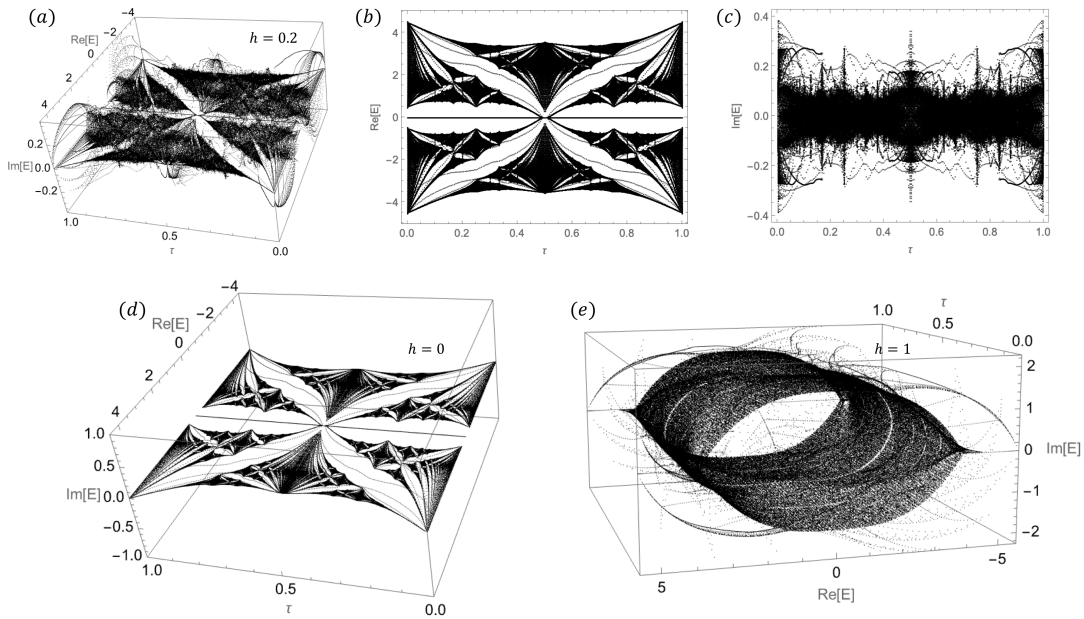

FIG. 3. Non-Hermitian analog to conventional Hofstadter butterfly. (a) Non-Hermitian Hofstadter butterfly plotted in three-dimensional space, $h = 0.2$. (b)-(c) Real/Imaginary eigenenergy projection of (a). (d) Hofstadter butterfly in the Hermitian limit. (e) Non-Hermitian Hofstadter butterfly plotted in three-dimensional space, $h = 1$. Zero modes are eliminated due to strong non-Hermiticity.

floquet operator (evolution operator over one driving period) can be approximated by

$$\hat{\mathcal{U}} \simeq e^{-\mathrm{i}\hat{H}((N-1)\Delta t)\Delta t} e^{-\mathrm{i}\hat{H}((N-2)\Delta t)\Delta t} \cdots e^{-\mathrm{i}\hat{H}(\Delta t)\Delta t} e^{-\mathrm{i}\hat{H}(0)\Delta t}, \tag{5}$$

which satisfies the Schrödinger equation $\hat{\mathcal{U}}(t + T, t)|\psi_\varepsilon(t)\rangle = e^{\mathrm{i}\varepsilon T}|\psi_\varepsilon(t)\rangle$, and the first quasienergy Brillouin zone is $\mathrm{Re}[\varepsilon] \in [\pi/T, \pi/T)$ with regard to time-periodicity [14]. The floquet modulation actually breaks the continuous translational symmetry in time, while discrete translational symmetry is preserved. Similar to real-space lattice system, we can slightly modify the Bloch theorem and obtain the Floquet-Bloch theorem, which applies to systems with periodic driving. By now it is obvious that floquet modulation can also extend the dimension by adopting a lattice in synthesis space-time dimensions.

A interesting phenomenon in floquet system is the anomalous bulk-boundary correspondence (aBBC) [15]. Induced by the periodic behavior of quasienergy, the gaps are ill-defined, so another type of in-gap topological modes emerges, called π modes. As shown in Fig. 4, the butterfly pattern holds roughly for real quasienergy spectrum when remaining other parameters unchanged as and setting $\omega = 2$. Aside from the zero modes, there are several bands consisted of in-gap topological modes believed to be π modes. The most amazing fact is, in static case, large non-Hermitian phase $h = 1$ can ruin zero modes, but they are recovered under $\omega = 2$ modulation.

CONCLUSION

We have constructed and analyzed a non-Hermitian quasiperiodic SSH ladder model, revealing rich topological phases and phase transitions driven by complex interchain coupling and quasiperiodicity. The model exhibits a metal-insulator transition characterized by a winding number, a non-Hermitian Hofstadter butterfly, and symmetry-stabilized zero modes. Each of these phenomena arises from the interaction among the bipartite nature of Hamiltonian, quasiperiodic modulation and non-Hermitian properties, presenting unique challenges and opportunities for observing novel phases.

Our findings contribute to the growing field of non-Hermitian topological systems and provide a helpful at-

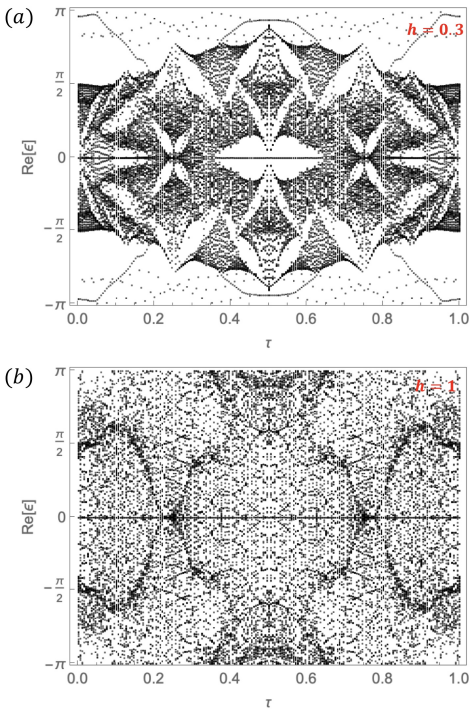

FIG. 4. Floquet Non-Hermitian Hofstadter butterfly. (a) Real part of quasienergy is plotted as a Non-Hermitian Hofstadter butterfly under floquet modulation, with frequency $\omega = 2$. Zero modes and π modes can be identified at $h = 0.3$. (b) Real part of quasienergy calculated with the same parameters as (a), except $h = 1$. Zero modes are recovered compared to its static counterpart.

tempt for exploring similar quasiperiodic models with complex potentials. Future work could explore variations in ladder geometry, the effect of higher-order couplings, and the role of floquet modulation. Knowing that both floquet formalism and quasiperiodicity are effective tools to extend the dimension, we may also apply them to investigate higher order topology.

We are grateful to Mengjie Yang, Zichang Hao for useful discussions. This manuscript only serves as the final project of PC5203.

Appendix A: Real-space Hamiltonian

We can rewrite the Hamiltonian in real-space,

$$H = \begin{pmatrix} T_1 & M & 0 & 0 & 0 & \cdots & 0 & 0 & M^\dagger \\ M^\dagger & T_2 & M & 0 & 0 & \cdots & 0 & 0 & 0 \\ 0 & M^\dagger & T_3 & M & 0 & \cdots & 0 & 0 & 0 \\ \cdots & \cdots & \cdots & \cdots & \cdots & \cdots & \cdots & \cdots & \cdots \\ 0 & 0 & 0 & 0 & 0 & ... & M^\dagger & T_{L-1} & M \\ M & 0 & 0 & 0 & 0 & ... & 0 & M^\dagger & T_L \end{pmatrix}, \tag{6}$$

where the blocks are

$$T_j = \begin{pmatrix} 0 & t_1 & \mu_{2j-1} & 0 \\ t_1 & 0 & 0 & \mu_{2j} \\ \mu_{2j-1} & 0 & 0 & t_2 \\ 0 & \mu_{2j} & t_2 & 0 \end{pmatrix}, \quad M = \begin{pmatrix} 0 & 0 & 0 & 0 \\ t_2 & 0 & 0 & 0 \\ 0 & 0 & 0 & 0 \\ 0 & 0 & t_1 & 0 \end{pmatrix}. \tag{7}$$

Appendix B: Wolfram Language code

Mathematica code for producing part of the results is uploaded on GitHub, which is publicly available in [16].

* phyuan@whu.edu.cn

[1] Y. Ashida, Z. Gong, and M. Ueda, Non-hermitian physics, Advances in Physics **69**, 249 (2020).
[2] W.-P. Su, J. R. Schrieffer, and A. J. Heeger, Solitons in polyacetylene, Physical review letters **42**, 1698 (1979).
[3] X.-J. Luo, J.-Z. Li, M. Xiao, and F. Wu, A family of third-order topological insulators from su-schrieffer-heeger stacking, arXiv preprint arXiv:2410.18016 (2024).
[4] H.-R. Xia, J.-Z. Li, S.-Y. Yuan, and M. Xiao, Photonic realization of chiral hinge states in a chern-insulator stack, arXiv preprint arXiv:2406.10637 (2024).
[5] P. G. Harper, Single band motion of conduction electrons in a uniform magnetic field, Proceedings of the Physical Society. Section A **68**, 874 (1955).
[6] L. Ge, Symmetry-protected zero-mode laser with a tunable spatial profile, Physical Review A **95**, 023812 (2017).
[7] J. D. Rivero and L. Ge, Chiral symmetry in non-hermitian systems: product rule and clifford algebra, Physical Review B **103**, 014111 (2021).
[8] J. Lyu, Z. Gao, L. Feng, and L. Ge, Non-hermitian gauged reciprocity and symmetry, Physical Review B **110**, 134102 (2024).
[9] Y. Liu, X.-P. Jiang, J. Cao, and S. Chen, Non-hermitian mobility edges in one-dimensional quasicrystals with parity-time symmetry, Physical Review B **101**, 174205 (2020).
[10] Y. Liu, Q. Zhou, and S. Chen, Localization transition, spectrum structure, and winding numbers for one-dimensional non-hermitian quasicrystals, Physical Review B **104**, 024201 (2021).
[11] S. Longhi, Topological phase transition in non-hermitian quasicrystals, Physical review letters **122**, 237601 (2019).
[12] K. Padavić, S. S. Hegde, W. DeGottardi, and S. Vishveshwara, Topological phases, edge modes, and the hofstadter butterfly in coupled su-schrieffer-heeger systems, Physical Review B **98**, 024205 (2018).
[13] R. B. Diener, G. A. Georgakis, J. Zhong, M. Raizen, and Q. Niu, Transition between extended and localized states in a one-dimensional incommensurate optical lattice, Physical Review A **64**, 033416 (2001).

[14] L. Zhou and D.-J. Zhang, Non-hermitian floquet topological matter—a review, Entropy **25**, 1401 (2023).
[15] M. S. Rudner, N. H. Lindner, E. Berg, and M. Levin, Anomalous edge states and the bulk-edge correspondence for periodically driven two-dimensional systems, Physical Review X **3**, 031005 (2013).
[16] S.-Y. Yuan, Code for non-hermitian quasiperiodic ssh ladder, `https://github.com/Siyu-Yuan/nH_SSH_ladder.git` (2024).